

Field Condition Reliability Assessment for SnPb and SnAgCu Solder Joints in Power Cycling Including Mini Cycles

Min Pei¹, Xuejun Fan² and Pardeep K. Bhatti²

¹Georgia Tech, 801 Ferst Dr. NW, Atlanta, GA 30332-0405

²Intel Corporation, M/S CH5-263, 5000 W Chandler Blvd, Chandler, AZ 85226
gte570t@prism.gatech.edu

Abstract

Actual field conditions that computer components such as microprocessors experience are different from the accelerated thermal cycling tests typically used to perform reliability assessment. Field conditions can include longer dwell times, different temperature ramp rates driven by power ON/OFF events, and temperature fluctuations during the power ON state due to workload patterns. Series of numerical simulations have been performed to study the effect of the field conditions on the solder joint fatigue life of electronic packaging. The simulation results show that SnPb and SnAgCu solders respond differently with respect to dwell time and mini cycles. Without considering the effect of mini-cycles, it is possible that SnAgCu may fail earlier than SnPb with very long dwell time. However, it is important to note if mini-cycles contribute to damage as seen in this analysis, the SnPb solder will probably still fail before SnAgCu solder.

Introduction

Electronic components continue to enter new product applications and markets, while design-to-production cycle is becoming shorter. The reliability of electronic components is usually studied with accelerated tests to reduce the validation time. Specifically for solder joint low-cycle fatigue, a commonly used test is accelerated thermal cycling. However the relationship between field conditions and the accelerated thermal cycling test is not well understood. This is especially true for newer product applications and markets. Simulation can be used to bridge this gap and to investigate the effect of various field condition parameters on reliability.

For server and desktop computer applications, there are 4 significant differences between the field conditions and accelerated thermal cycling test: 1) field conditions have longer dwell times at low and high temperatures (few ON/OFF cycles per day or per week, depending on the market application) than thermal cycle test condition (usually 20-60 minutes/cycle); 2) temperature change driven by power ON/OFF events has a different ramp rate compared to the thermal cycling test performed in a chamber; 3) temperature gradients exist in the electronic package in field conditions; and 4) temperature fluctuates during the power ON state driven by workload patterns. The temperature range of these fluctuations, called “mini-cycles” is much smaller than temperature fluctuations caused by power ON/OFF cycles, but the frequency can be much higher.

Sahasrabudhe et al. [1] conducted a series of tests to identify the impact of dwell time on cycles to failure for the second-level solder joint interconnect. Their experimental results showed that the fatigue life of eutectic SnPb solder joints decreases significantly when the dwell time is increased from 15 minutes to 30 minutes and then 90 minutes. Zhai et

al. [2] studied the effects of ramp rate and dwell time through laboratory results and design of experiments (DOE) using finite element analysis (FEA). Fan et al. [3], Yoon et al. [4], and Lau et al. [5] also investigated the ramp rate and dwell time effect for lead-free solders. These studies revealed that comprehending the ramp rate and dwell time effect can help in fully exploiting the field condition based reliability evaluation methodology. However, to the best knowledge of the authors, very little research has been done to determine the impact of mini-cycles on the fatigue life of solder joints. Dishongh et al. [6] used laser interferometry to measure the residual deformation of solder joints to study the effect of mini-cycles. The deformation field of the package was measured at a cross section at the end of each cycle. These test results showed that the shear strain in solder joints in temperature cycling with mini cycles is slightly smaller than that without mini cycles.

This paper investigates the damage generated in field conditions, and their effect on fatigue failure of electronic packaging, by performing numerical simulations using FEA on both eutectic SnPb solder and SnAgCu lead-free solders under power cycling with mini cycles. This paper also examines the superposition method, which can significantly improve the computational efficiency to account for the effect of mini-cycles.

Finite Element Model

Flip-chip Ball Grid Array (FC-BGA) is a common packaging technology used in computer applications today. A typical BGA package was modeled with finite element method using ABAQUS and is shown in Figure 1.

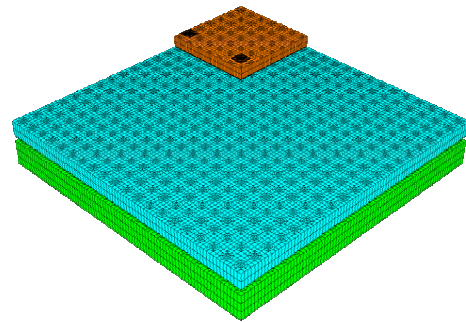


Figure 1: FEA mesh of a FC-BGA package

A quarter of the package is simulated and the symmetry boundary condition is applied. This study will concentrate on the deformation of second level interconnection (SLI) solder joint between the BGA substrate and the PCB. 3D solid linear element with reduced-integration (C3D8R) is used [14]. The model includes silicon die, underfill layer, BGA substrate,

PCB, and copper pads on both the BGA substrate and the PCB. The solder joints are modeled as solder mask defined (SMD) on substrate side and metal defined (MD) on PCB side. Two different mesh density patterns are used to model the solder balls, as shown in Figure 2. The refined mesh pattern is used at the location of interest (e.g. the location of first failure) and the coarse mesh is used in the rest of the model to conserve computing resources. The refined solder joint mesh includes a 25 micron thick region (with 2 layers of elements) at each solder/copper pad interface. The stresses and strains are volumetrically averaged within these 2 regions to overcome the edge stress singularity at the interface [7][8] [14].

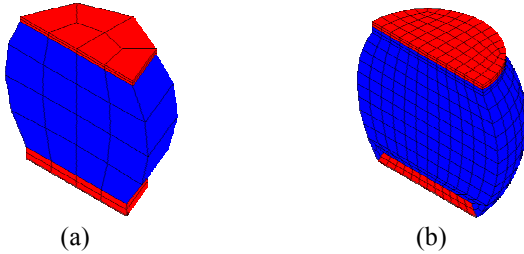


Figure 2: Details of solder ball coarse and refined mesh patterns

Material Properties

There is considerable variation in the published test data on mechanical properties of solder due to tolerances in the measurement equipment/techniques and variability in test specimen design and preparation. This has led to development of several constitutive material models for plasticity and steady state creep behavior of SnPb and SnAgCu solders. One difficulty has been the separation of time-independent (plastic) and time-dependent (creep) inelastic components from the measured strains. A combined creep and plasticity material model, which captures the total strain behavior in the operating range, was proposed by Wong, Helling, and Clark for 63Sn37Pb eutectic alloy [9]. Bhatti et al. [10][11][12] implemented this constitutive model and developed 3-dimensional package level finite element models to perform solder joint creep simulations. This material model can be written as

$$\dot{\epsilon} = \frac{\dot{\sigma}}{E} + B_1 D \left(\frac{\sigma}{E} \right)^3 + B_2 D \left(\frac{\sigma}{E} \right)^7 \quad (1)$$

where

$\dot{\epsilon}$ = Total strain rate (1/sec)

σ = Stress (MPa)

E = Modulus of Elasticity (MPa) = 56000 – 88T

T = Temperature (K)

$B_1 = 1.70 \times 10^{12}$ 1/sec

$B_2 = 8.90 \times 10^{24}$ 1/sec

$$D = \exp\left(\frac{-5413}{T}\right)$$

The second term in the equation (1) accounts for the grain boundary sliding (GBS) creep strain, and the third term in the equation accounts for the matrix creep (MC) strain.

Wiese et al. [12] studied the creep behavior of bulk, PCB samples, and flip chip solder joint samples of Sn4.0Ag0.5Cu solder and identified two mechanisms for steady state creep deformation for the bulk and PCB samples. They attributed these to climb controlled (low stress) and combined glide/climb (high stress) mechanisms and represented steady state creep behavior using a double power law model as shown below

$$\dot{\epsilon} = \frac{\dot{\sigma}}{E} + A_1 D_1 \left(\frac{\sigma}{\sigma_n} \right)^3 + A_2 D_2 \left(\frac{\sigma}{\sigma_n} \right)^{12} \quad (2)$$

where

$\dot{\epsilon}$ = Total strain rate (1/sec)

σ = Stress (MPa)

E = Elastic Modulus (MPa) = 59533 – 66.667T

T = Temperature (K)

$A_1 = 4.0 \times 10^{-7}$ 1/sec

$A_2 = 1.0 \times 10^{-12}$ 1/sec

$$D_1 = \exp\left(\frac{-3223}{T}\right)$$

$$D_2 = \exp\left(\frac{-7348}{T}\right)$$

$\sigma_n = 1$ MPa

The second term in the equation (2) represents the climb controlled creep strain and the third term represents the combined glide/climb strain. Syed [7] applied this creep model to establish the fatigue life model for SnAgCu solders.

Published material properties [7] are used for all other materials as listed in Table 1..

Table 1 material constants

Material	Young's Modulus (GPa)	Poisson's Ratio	Coefficient of Thermal Expansion (ppm/°C)
Silicon	131.0	0.3	2.6
Copper	128.7	0.3435	17.0
Underfill	9.9	0.23	24.0
Substrate	22.0	0.11	17.0
PCB	24.2	0.11	19.6
SnPb			25.5
SnAgCu			20.0

Thermal Cycling Loading Conditions

Isothermal condition in the BGA package is assumed. To simulate the field condition, two different temperature profiles are applied to the model. First, the power ON/OFF cycle is assumed to range from 25°C to 90°C, with the total per-cycle time of 24 hours, as shown in Figure 3. The ON and OFF state are 16 hours and 8 hours, respectively, with 1 minute ramp time in each transition. Such a profile can help to understand the effect of ramp time and long dwell time on solder joint damage.

Second, the mini cycles are considered during ON state, as shown in Figure 4. The length of each mini cycle is assumed to be 12 minutes. Therefore, there are total 80 mini cycles for a 16-hour ON period. The details of the mini cycle are plotted in Figure 5. When mini cycles are considered during power cycles, the finite element simulation will run through all 80 mini cycles in the ON state during each power cycle. This requires significant amount of computational resources and time. However, this is necessary to understand how mini cycles affect the solder joint reliability compared to the power cycle without mini cycles.

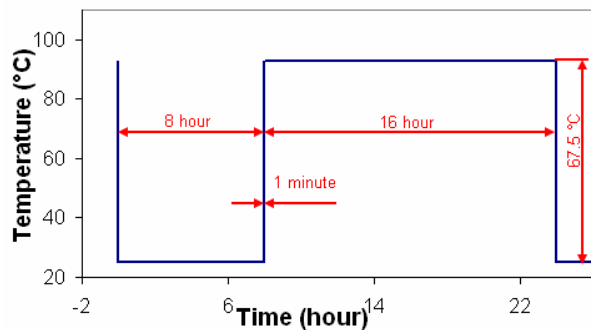


Figure 3: Power cycle profile without mini cycles

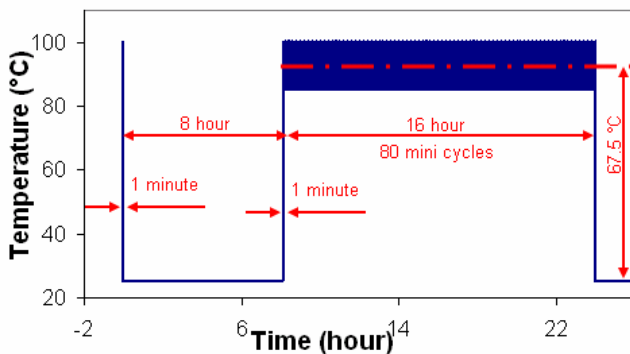


Figure 4: Power cycle profile with mini cycles

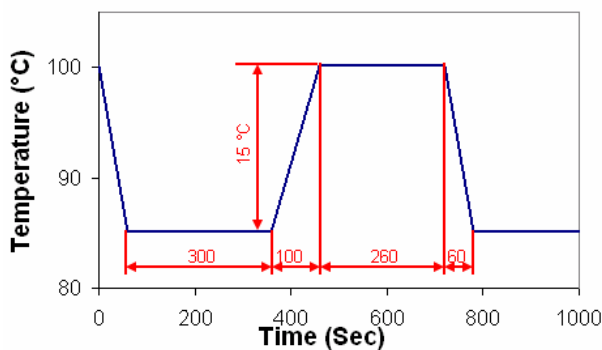


Figure 5: Mini cycle profile

Power Cycle Condition without Mini Cycles

A total of 10 power cycles (total physical time: 10 days) were simulated without considering mini cycles first. Figure 6 and Figure 7 plot the time-history of averaged cumulated equivalent creep strain (denoted by CEEQ) and the averaged

cumulated creep energy density (ECDDEN) at package side, respectively, for SnPb and SnAgCu solders. The temperature profile is also shown in these figures with light green line. Analysis shows that the per-cycle CEEQ and per-cycle ECDDEN stabilized within two or three cycles for both solder materials. This suggests that 3 cycles will be sufficient in similar studies in the future.

As expected, from Figure 6 and Figure 7, the creep strain accumulation in SnPb is much faster than in SnAgCu, because SnPb is softer and has higher creep strain rates than SnAgCu in the temperature range investigated. However, it should be noted that the creep limit of SnPb is also much higher than SnAgCu.

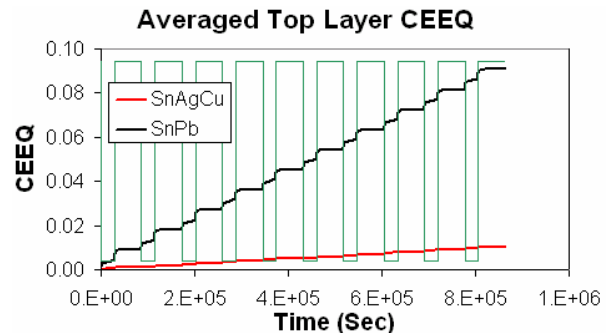


Figure 6: Averaged CEEQ history under power cycle without mini cycles

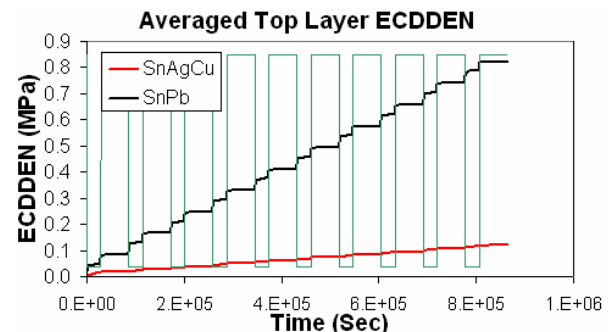


Figure 7: Averaged ECDDEN history under power cycle without mini cycles

Further, in order to understand the effect of dwell time and ramp rate, the CEEQ and ECDDEN accumulation in one cycle (the 10th cycle) are plotted in Figures 8-11. It is noted that, unlike what we observe in accelerated test condition simulations [3], the majority of creep for both solder materials is accumulated during dwell times. This suggests that the dwell time is a dominant factor in the field condition reliability assessment.

Two solder alloys respond differently in creep accumulation during the long dwell time. Because the SnPb solder has higher creep rate, especially at high temperatures, the creep accumulation reaches an asymptotic value at high temperature after a few hours (shown in Figure 8). The stress is quickly relaxed and creep accumulation is slowed with longer dwell time. The Von Mises stress plot in Figure 12 confirms that stress is almost relaxed for SnPb at high temperature after a certain period of time. But the stress is not

fully relaxed at low temperature dwell period, and the creep strain continues to accumulate after 8 hours.

SnAgCu solder, on the other hand, is stiffer and has lower creep rate. Even after 16 hours dwell time at high temperature, Figure 9 shows that the creep continues to accumulate and the asymptotic value is not yet reached. The Von Mises stress plot in Figure 13 shows that the residual stress remains at a relative high level. At low temperature dwell period, though the stress has undergone some degree of relaxation, the level is rather high. Therefore, significant creep accumulation occurs during the low temperature dwell period.

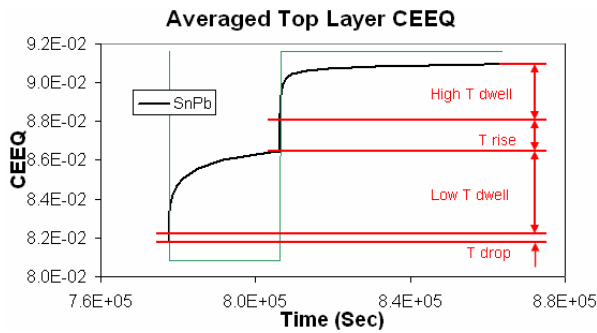


Figure 8: Averaged CEEQ history during 10th cycle, SnPb solder

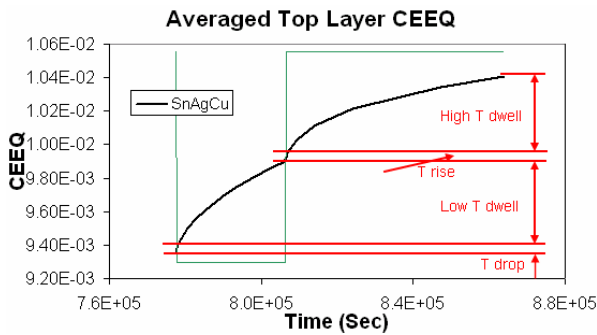


Figure 9: Averaged CEEQ history during 10th cycle, SnAgCu solder

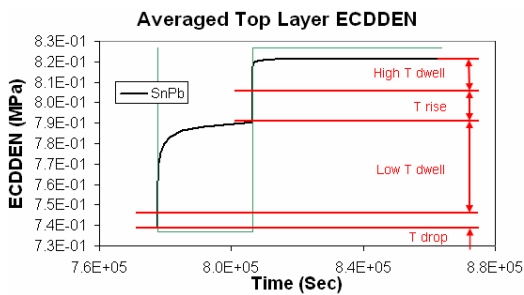


Figure 10: Averaged ECDDEN history during 10th cycle, SnPb solder

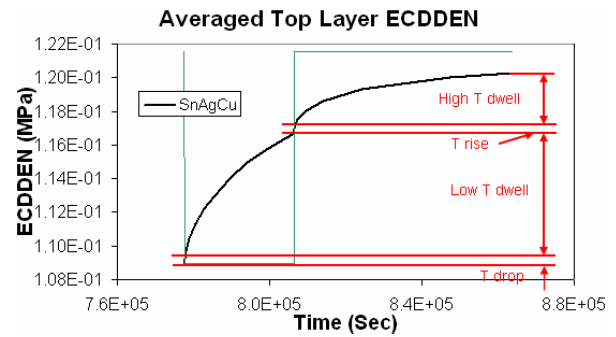


Figure 11: Averaged ECDDEN history during 10th cycle, SnAgCu solder

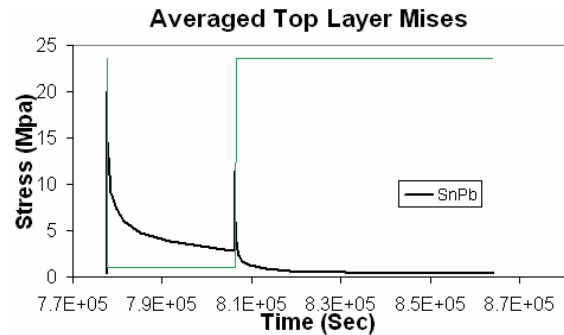


Figure 12: Averaged Mises stress history during 10th cycle, SnPb solder

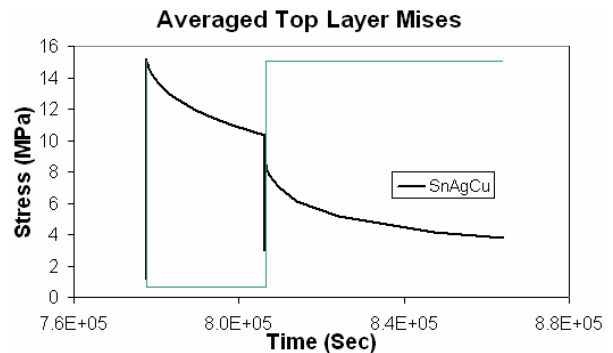


Figure 13: Averaged Mises stress history during 10th cycle, SnAgCu solder

In summary, unlike conventional accelerated thermal cycling test conditions, this simulation shows that in power cycling without mini-cycles, the majority of creep accumulation occurs during the dwell time, rather than during the ramp periods. This can be explained by the very rapid ramp rates we assumed for the field condition, which don't give solder enough time to creep during ramp times, and much longer dwell times. Furthermore, SnPb solder almost completely relaxes stresses during the ON state, but SnAgCu still has significant stress left even after 16 hours dwell. During the OFF state, both solder alloys are continuously stress relaxing even after 8 hours dwell without reaching a stress-free state. These results suggest that it is possible that SnAgCu may fail earlier than SnPb if the ON state dwell time increases beyond some threshold value. However, it is important to note that the effect of mini cycles has not been considered up to this point.

Power Cycle Condition with Mini Cycles

As shown in Figure 5, each power cycle is assumed to consist of 80 mini cycles during the ON state. Figure 14 plots the history of the averaged CEEQ in the first two power cycles with and without mini cycles for SnPb solder. Unexpectedly, the creep strain keeps increasing during mini cycles. The total per-power-cycle accumulated creep strain with mini-cycles is almost 4× the one without mini cycles. The results suggest that the SnPb solder experiences significant creep accumulation during the ON state due to temperature fluctuations. Such an observation can be explained from the Von Mises stress plot, shown in Figure 15. It can be seen that for SnPb solder, the stress stays at a higher level due to mini-cycling. Each temperature fluctuation serves as a re-loading procedure to maintain the stress level, thus continuing creep accumulation. Figure 16 gives the Von Mises stress plot in one mini cycle.

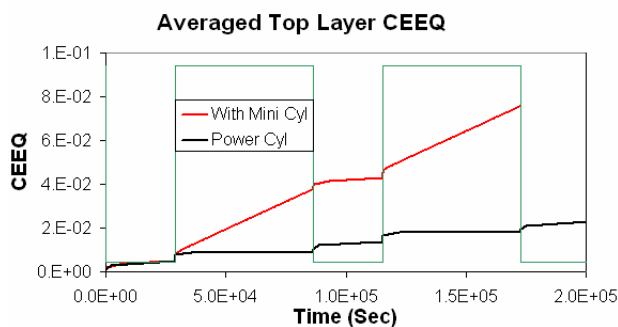


Figure 14: Averaged CEEQ history under power cycle with and without mini cycles, SnPb solder

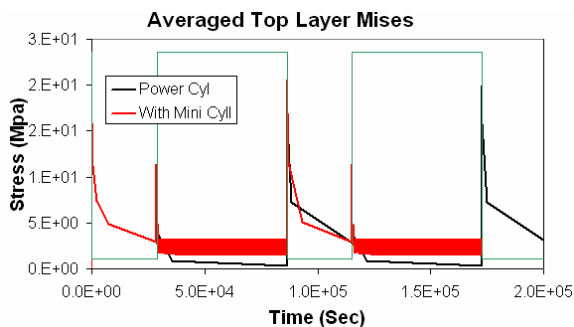


Figure 15: Averaged Von Mises stress history under power cycle with and without mini cycles, SnPb solder

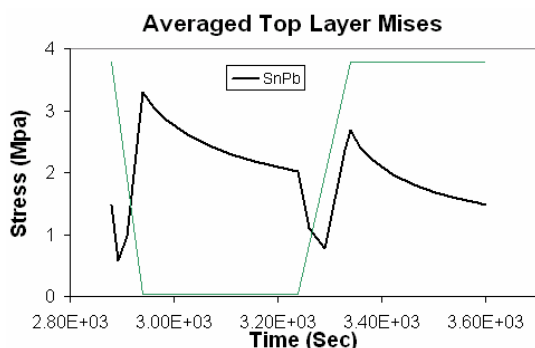


Figure 16: Von Mises stress during one mini cycle, SnPb solder

Figure 17 plots three power cycles with and without mini cycles for SnAgCu solder. Unlike SnPb, the mini cycles do not have a significant contribution to creep accumulation for SnAgCu. From the Von Mises stress plot in Figure 18, it can be seen that temperature fluctuations during the high temperature dwell period do not increase the stress level because SnAgCu is more creep resistant. Figure 19 shows Von Mises stress plot in one mini cycle. It can be seen that there is almost no softening during dwell time of the mini cycle, and no reloading occurs when temperature changes.

This analysis suggests that if mini-cycles are considered, the SnPb solder will probably still fail before SnAgCu solder in the simulated field condition.

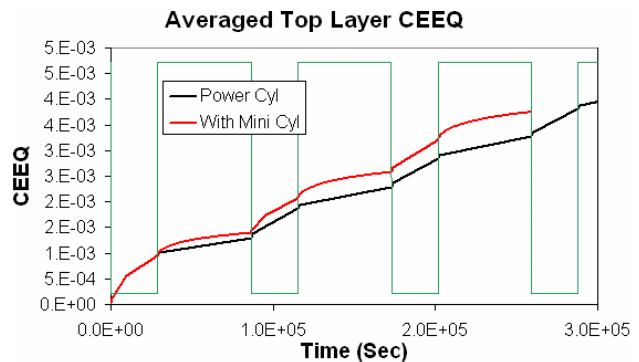


Figure 17: Averaged CEEQ history under power cycle with and without mini cycles, SnAgCu solder

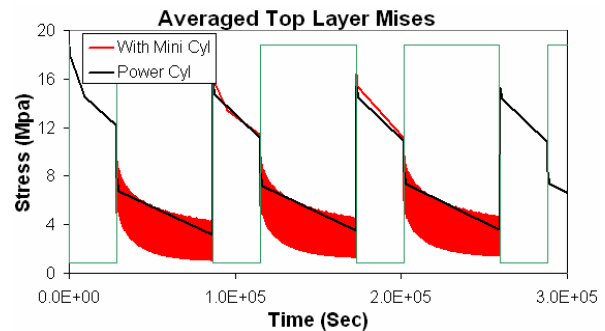


Figure 18: Averaged Von Mises stress history under power cycle with and without mini cycles, SnAgCu solder

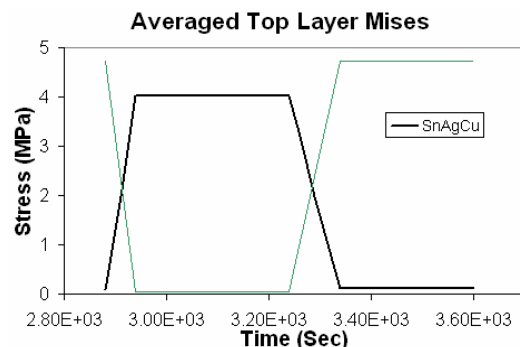


Figure 19: Von Mises stress during one mini cycle, SnAgCu solder

Superposition Method

It's very time consuming to simulate a power cycle profile with mini-cycles because finite element simulation needs to run through dozens of mini cycles (e.g., 80 mini cycles in our study) to complete one power cycle. The superposition method can be effectively used to simulate this case by combining the results of individual power cycle and mini-cycle analyses.

The mini cycle shown in Figure 5 is simulated without the power cycle, with the assumption of stress-free temperature as the maximum temperature during mini-cycle (e.g. 100°C in our study). It usually takes two to three cycles to obtain the stabilized per-cycle CEEQ. The readers can refer to reference [14] for a detailed discussion on the initial stress-free temperature assumption.

The following equation is used to estimate the per-power-cycle CEEQ using superposition method,

$$\text{Per-power-cycle CEEQ with mini cycles} = \text{Per-power-cycle CEEQ without mini cycles} + n \times \text{per-mini-cycle CEEQ} \quad (3)$$

where n is the number of mini cycles in a power cycle.

The above equation is also applied to estimate the per-power-cycle results. Table 2 gives the relative errors for accumulated CEEQ and ECDDEN compared to the results from power cycle with mini cycles. For SnPb solder, the superposition method has relative error of less than 1% for both cumulated creep strain and creep energy density. For SnAgCu solder, the superposition method has 2% of relative error on cumulated strain but have 18% of relative errors on creep energy density. Therefore the superposition method can be used as a quick way to estimate the effect of mini cycles and results in computational time reduction by more than a factor of 10.

Table 2: Relative error by superposition method

	Relative Error of Superimpose (%)	
	SnPb	SnAgCu
CEEQ per cycle	0.6	2.1
ECDDEN per cycle	0.7	18.2

Mini Cycles at a Lower Temperature

When an electronic component such as a microprocessor is in the stand-by mode, the temperature is normally in a lower temperature range. In this section we investigate a field condition for mini cycles with the assumed temperature range of 45°C to 55°C. The superposition method is applied to assess the effect of these mini cycles.

Figure 20 shows the lumped effect of 80 mini cycles compared to the per-cycle CEEQ in one power cycle only for SnPb solder. It can be seen that the per-cycle CEEQ of 80 low temperature mini cycles accumulate only 24% of the CEEQ of one power cycle. This number is significantly lower than the results for high-temperature mini cycles, where the mini cycles contribute 3× of that in power cycle only condition. For SnAgCu solder, the 80 low temperature mini cycles accumulate only 1.7% of CEEQ of power cycle, as shown in Figure 21.

These results demonstrate that the contribution of mini cycles is highly dependent on the mean and the range of the temperature fluctuation.

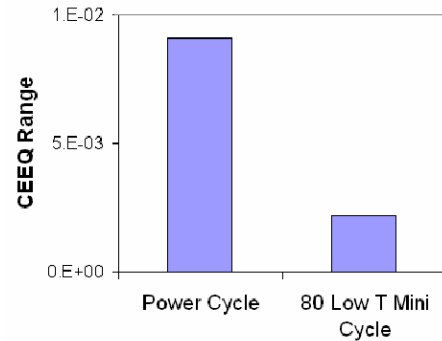


Figure 20: Mini cycle CEEQ accumulation at lower temperature, SnPb Solder

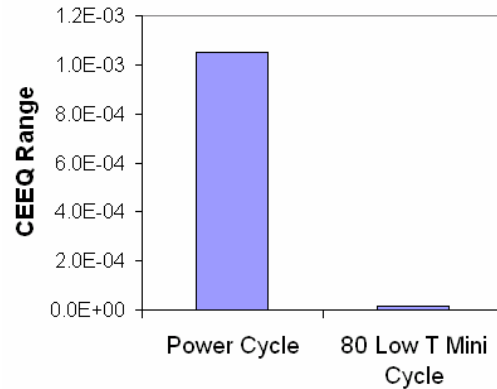


Figure 21: Mini cycle CEEQ accumulation at lower temperature, SnAgCu solder

Summary

Finite element modeling of a FC-BGA package is performed to assess the solder joint reliability under an assumed power cycling with mini cycles field condition. For SnPb solder, the results show that the creep strain accumulated during power cycling with mini-cycles is significantly higher than that without mini cycles. The mini-cycles contribute about 3× to the total creep strain accumulation compared to the power cycling only condition. However, for SnAgCu, the mini-cycles contribute only about 12% to the total creep strain. This implies that SnPb solder experiences significant creep and stress relaxation due to mini-cycle loading while more creep resistant SnAgCu is not sensitive to mini-cycles.

Unlike conventional accelerated thermal cycling test conditions, this simulation shows that in power cycling without mini-cycles, the majority of creep accumulation occurs during the dwell time, rather than during the ramp periods. Furthermore, SnPb solder almost completely relaxes stresses during the ON state, but SnAgCu still has significant stress left even after 16 hours dwell. During the OFF state, both solder alloys are continuously stress relaxing after 8 hours dwell without reaching an asymptotic value. These results suggest that without considering the effect of mini-cycles, it is possible that SnAgCu may fail earlier than SnPb

when a certain threshold value of ON state dwell time is exceeded. However, if the mini-cycles contribute to damage as observed in this analysis, the SnPb solder will probably still fail before the SnAgCu solder for the FCBGA package considered in this study.

Finally, superposition method can be used effectively to estimate the effect of mini cycles. The superposition method was applied to study the effect of mini cycles at a lower temperature. Results show that mini cycles have a much smaller contribution when temperature fluctuation level is lower. Further experimental studies are needed to validate the results of this study.

Acknowledgments

The authors would like to thank Shubhada Sahasrabudhe, Eric Monroe and Patrick Counihan at Intel Corporation for their input and support of this effort.

Reference

- [1] Shubhada Sahasrabudhe, Eric Monroe, Shalabh Tandon, Mitesh Patel, "Understanding the Effect of Dwell Time on Fatigue Life of Packages Using Thermal Shock and Intrinsic Material Behavior", 2003 Electronic Components and Technology Conference (ECTC), 898-904.
- [2] Zhai, C., Sidharth, and Blish, R., "Board Level Solder Reliability Versus Ramp Rate and Dwell Time During Temperature Cycling," *IEEE Transactions On Device Reliability and Material Reliability*, Vol. 3, No. 4, December 2003. pp. 207-212.
- [3] Xuejun Fan, George Raiser, Vasu S. Vasudevan, Effects of Dwell Time and Ramp Rate on Lead-Free Solder Joints in FCBGA Packages, 2005 Electronic Components and Technology Conference (ECTC), 901-906.
- [4] S. Yoon, Z. Chen, M. Osterman, B. Han and A. Dasgupta Effect of Stress Relaxation on Board Level Reliability of Sn Based Pb-Free Solders 2005 Electronic Components and Technology Conference (ECTC), 1210-1214.
- [5] John Lau and Walter Dauksher, "Effects of Ramp-Time on the Thermal-Fatigue Life of SnAgCu Lead-Free Solder Joints", 2005 Electronic Components and Technology Conference (ECTC), 1292-1298.
- [6] Terry Dishongh, Cemal Basaran, Alexander N. Cartwright, Ying Zhao and Heng Liu, "Impact of Temperature Cycle Profile on Fatigue Life of Solder Joints", *IEEE Transactions on Advanced Packaging*, Vol. 25, No, 3, pp. 433-438, 2002
- [7] Syed, A R, Accumulated Creep Strain and Energy Density Based Thermal Fatigue Life Prediction Models for SnAgCu Solder Joints, ECTC 2004
- [8] Syed, A., "Predicting Solder Joint Reliability for Thermal, Power, & Bend Cycle within 25% Accuracy," 51st ECTC 2001, pp. 255-263.
- [9] Wong, B., Helling D.E., Clark, R.W., A creep-rupture model for two-phase eutectic solders, *IEEE Transactions on CMPT*, Vol. 11, No. 3, September, 1988, 284-290.
- [10] Bhatti, P K, Gschwend. K., Kwang, A.Y. Syed, A.R., Three-dimensional creep analysis of solder joints in

surface mount devices, *ASME Journal of Electronic Packaging*, March 1995, 117, 20-26.

- [11] Bhatti, P K, Gschwend. K., Kwang, A.Y. Syed, A.R., Computer simulation of leaded surface mount devices and solder joints in a thermal cycling environment, *EEP-Vol. 4-2, Advances in Electronic Packaging*, ASME, 1993, 1047 -1054
- [12] Bhatti, P K, Gschwend. K., Effect of global and local CTE mismatch on solder joint creep in SMT devices, *EEP – Vol. 8, Structural analysis in microelectronics and fiber optics*, ASME 1994, 55-63.
- [13] Wiese, S., et al, "Microstructural Dependence of Constitutive Properties of Eutectic SnAg and SnAgCu Solders," 53rd ECTC 2003, pp. 197-206.
- [14] Xuejun Fan, Min Pei, and Pardeep K. Bhatti, Effect of Finite Element Modeling Techniques on Solder Joint Fatigue Life Prediction of Flip-Chip BGA Packages, To be published in ECTC 2006